

Evolution of superconductivity and antiferromagnetic order in $\text{Ba}(\text{Fe}_{0.92-x}\text{Co}_{0.08}\text{V}_x)_2\text{As}_2$

Jieming Sheng,^{1,2,3,4} Xingguang Li,¹ Congkuan Tian,¹ Jianming Song,⁵ Xin Li,⁵ Guangai Sun,⁵ Tianlong Xia,¹ Jincheng Wang,¹ Juanjuan Liu,¹ Daye Xu,¹ Hongxia Zhang,¹ Xin Tong,^{2,3} Wei Luo,^{2,3} Liusuo Wu,⁴ Wei Bao,^{1,6} and Peng Cheng¹

¹*Department of Physics and Beijing Key Laboratory of Opto-electronic Functional Materials & Micro-nano Devices, Renmin University of China, Beijing 100872, P. R. China*

²*Institute of High Energy Physics, Chinese Academy of Sciences (CAS), Beijing 100049, China*

³*Spallation Neutron Source Science Center, Dongguan 523803, China*

⁴*Department of Physics, Southern University of Science and Technology, Shenzhen 518055, China*

⁵*Key Laboratory of Neutron Physics and Institute of Nuclear Physics and Chemistry, China Academy of Engineering Physics, Mianyang 621999, China*

⁶*Department of Physics, City University of Hong Kong, Kowloon, Hong Kong SAR*

(Dated: January 29, 2020)

The vanadium doping effects on superconductivity and magnetism of iron pnictides are investigated in $\text{Ba}(\text{Fe}_{0.92-x}\text{Co}_{0.08}\text{V}_x)_2\text{As}_2$ by transport, susceptibility and neutron scattering measurements. The doping of magnetic impurity V causes a fast suppression of superconductivity with T_c reduced at a rate of 7.4 K/1%V. On the other hand, the long-range commensurate C -type antiferromagnetic order is recovered upon the V doping. The value of ordered magnetic moments of $\text{Ba}(\text{Fe}_{0.92-x}\text{Co}_{0.08}\text{V}_x)_2\text{As}_2$ follows a dome-like evolution versus doping concentration x . A possible Griffiths-type antiferromagnetic region of multiple coexisting phases in the phase diagram of $\text{Ba}(\text{Fe}_{0.92-x}\text{Co}_{0.08}\text{V}_x)_2\text{As}_2$ is identified, in accordance with previous theoretical predictions based on a cooperative behavior of the magnetic impurities and the conduction electrons mediating the Ruderman-Kittel-Kasuya-Yosida interactions between them.

INTRODUCTION

Antiferromagnetic (AFM) correlations are closely related to the unconventional superconductivity (SC) in Fe-based superconductors[1, 2]. The typical parent compound BaFe_2As_2 (122) exhibits a collinear C -type AFM order and orthorhombic lattice distortion below $T_N \sim 138$ K, and superconductivity gradually emerges with suppressing both the AFM and structural transitions with charge doping[3, 4]. At the same time, the evolutions of AFM order with chemical doping present rich features. For example, the AFM order changes from long-range commensurate to short-range transversely incommensurate with Co/Ni electron doping and finally disappears with the avoidance of magnetic quantum critical point (QCP)[5, 6]. On the other hand, hole doping on the Ba site with alkali metals could induce a tetragonal magnetic phase with spin-reorientation and a new double-Q AFM order[7, 8]. Moreover hole doping on the Fe site with magnetic impurities Cr/Mn could generate a competing G-type AFM order and spin fluctuations[9, 10]. The above observations show the diverse responses of Fe-based magnetism to different impurities and have been considered as valuable clues to the puzzle of Fe-based superconducting mechanism, which has not yet been solved. Exploring new impurity effect therefore is called for.

The Vanadium impurity doping effect on iron pnictides has been rarely studied until recently. In a previous work, we found that vanadium serves as magnetic impurity and a very effective hole donor for the 122 system[11]. The avoided QCP and spin glass state which were previously reported in the superconducting phase of Co/Ni-doped BaFe_2As_2 can also be realized in non-superconducting $\text{Ba}(\text{Fe}_{1-x}\text{V}_x)_2\text{As}_2$ [11]. A very recent transport and spectroscopy investigation on V-

doped BaFe_2As_2 found evidence for coexistence of AFM and local superconducting regions[12]. These experimental findings make vanadium an interesting impurity probe for further investigations. So far the studies of vanadium impurities only focused on the parent compound BaFe_2As_2 . The influences on the superconductivity in FeAs-122 system is still unknown.

In this paper, we report the physical properties of $\text{Ba}(\text{Fe}_{0.92-x}\text{Co}_{0.08}\text{V}_x)_2\text{As}_2$, which explore the effect of magnetic impurity V on the $\text{Ba}(\text{Fe}_{0.92}\text{Co}_{0.08})_2\text{As}_2$ superconductor with near optimal $T_c \approx 22$ K. Besides a fast suppression of superconductivity, V doping could tune the short-range incommensurate AFM order back to a long-range commensurate one. The onset AFM ordering temperature identified from neutron scattering measurements can be greatly enhanced (>70 K) at some certain doping concentration, indicating possible new magnetic phases. Finally the phase diagram of $\text{Ba}(\text{Fe}_{0.92-x}\text{Co}_{0.08}\text{V}_x)_2\text{As}_2$ is given and the underlying physics is discussed.

EXPERIMENTAL DETAILS

Single crystals of $\text{Ba}(\text{Fe}_{0.92-x}\text{Co}_{0.08}\text{V}_x)_2\text{As}_2$ were grown by self-flux method similar to our previous report[11]. Crystals with nominal doping between $x = 0$ and $x = 0.32$ are obtained for x-ray, magnetization, electrical transport and neutron scattering measurements. The x-ray diffraction patterns were collected from a Bruker D8 Advance x-ray diffractometer using Cu K_α radiation. The magnetization measurements of our samples were performed using a Quantum Design MPMS3. Resistivity measurements were performed on a Quantum Design physical property measurement system (QD PPMS-14T).

Neutron scattering experiments were carried out on

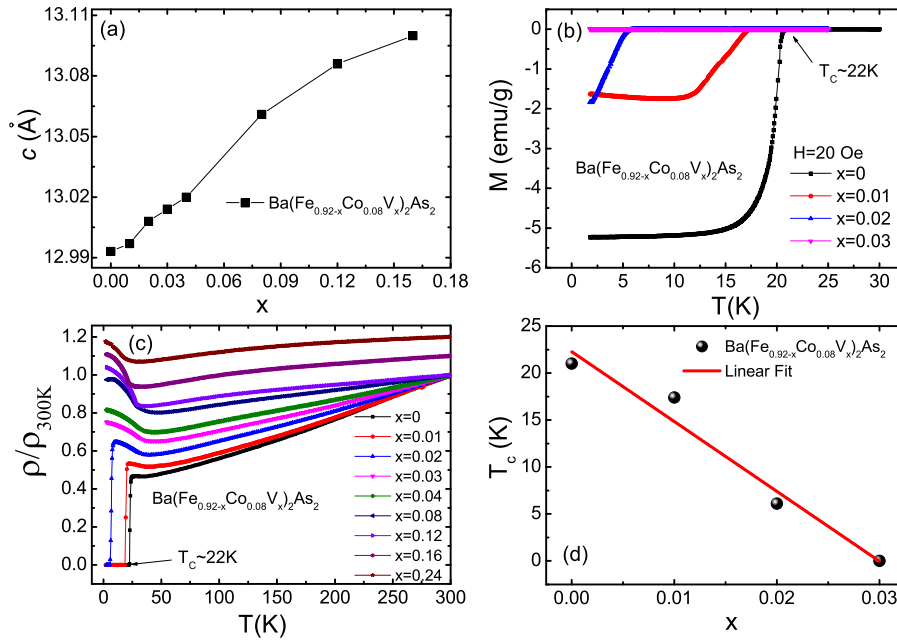


FIG. 1: (a) Room temperature c -axis lattice parameters of the $\text{Ba}(\text{Fe}_{0.92-x}\text{Co}_{0.08}\text{V}_x)_2\text{As}_2$ series as a function of nominal V concentration x . (b) Temperature dependence of zero-field-cooling magnetic susceptibilities for $x=0-0.03$ samples under a field of 20 Oe. (c) Temperature dependence of electrical resistivity for $\text{Ba}(\text{Fe}_{0.92-x}\text{Co}_{0.08}\text{V}_x)_2\text{As}_2$, the data are normalized to the room temperature value. For $x=0.16$ and $x=0.24$, the data are shifted by a constant value of 0.1 and 0.2 respectively for clarity. (d) The superconducting transition temperature T_c is plotted as a function of V doping concentration. The red solid line is the linear fitting result of the data.

‘Xingzhi’ cold neutron triple-axis spectrometer at China advanced research reactor (CARR)[13] and ‘Kunpeng’ cold neutron triple-axis spectrometer at China Academy of Engineering Physics (CAEP). The results below are all reported using the orthorhombic structural unit cell. For each doping, a single crystal with typical mass of 0.1~0.2 grams was aligned to the $(H\ 0\ L)$ scattering plane. For $x=0.12$, the crystal was also aligned in the $(0\ K\ L)$ scattering plane, allowing a search for possible incommensurate AFM phase along the b axis $((0\ K\ 0)$, transverse direction) similar as that in a previous report[5].

RESULTS

Fig. 1(a) presents the doping dependent c -axis lattice parameters of $\text{Ba}(\text{Fe}_{0.92-x}\text{Co}_{0.08}\text{V}_x)_2\text{As}_2$ derived from the single crystal x-ray data. Vanadium substitution effectively expands the c -axis similar as the effect that observed in $\text{Ba}(\text{Fe}_{1-x}\text{V}_x)_2\text{As}_2$ [11].

Fig. 1(b) shows the temperature dependence of DC magnetic susceptibilities for $x=0-0.03$ samples under a field of 20 Oe. For $x=0$, namely $\text{Ba}(\text{Fe}_{0.92}\text{Co}_{0.08})_2\text{As}_2$, the onset transition of the Meissner effect appears at 22 K. With slight V doping, both the superconducting transition temperature T_c and the superconducting shielding volume fraction quickly decrease. The fast suppression of superconductivity also manifests in the temperature dependent resistivity data (Fig. 1(c)).

T_c is defined as the onset point of Meissner effect which corresponds well with the zero-resistivity temperature determined from the R-T curve. The T_c suppression rate is calculated to be 7.4 K/1%V (Fig. 1(d)), similar as that in previous reports about magnetic impurity doped Fe-based superconductors such as V-doped LiFeAs [14], Cr-doped $\text{Ba}(\text{Fe,Ni})_2\text{As}_2$ [15] or Mn-doped $\text{Ba}_{0.5}\text{K}_{0.5}\text{Fe}_2\text{As}_2$ [16]. On the other hand, the phase diagram of $\text{Ba}(\text{Fe,Co})_2\text{As}_2$ has been extensively studied in early publications[5, 17], consensus has been reached about the existence of a weak short-range incommensurate AFM order in the slightly under doped region. According to the values of lattice parameter, T_c and transport properties, we can safely put our $\text{Ba}(\text{Fe}_{0.92}\text{Co}_{0.08})_2\text{As}_2$ sample in this region which have superconductivity at 22 K coexisting with a short-range incommensurate AFM order below 30 K.

The temperature dependent resistivities of all samples are shown in Fig. 1(c), an anomaly feature at around 30 K gradually emerges with increasing x . This anomaly quite resembles the resistivity anomaly caused by AFM/structural transition in Fe-based 122 materials, which indicates a possible recovery of stronger magnetic order in the samples. Therefore, as shown in Fig. 2, we measured the DC magnetic susceptibilities of the normal state for all samples with $H=1$ T applied parallel to the ab -plane. For $x=0$, the short-range incommensurate AFM order is too weak to generate an AFM feature in the susceptibility data. But for $x \geq 0.01$, the AFM transition features in the M-T curves emerge and get clearer and sharper with increasing x . The AFM transition temperature T_N shown in

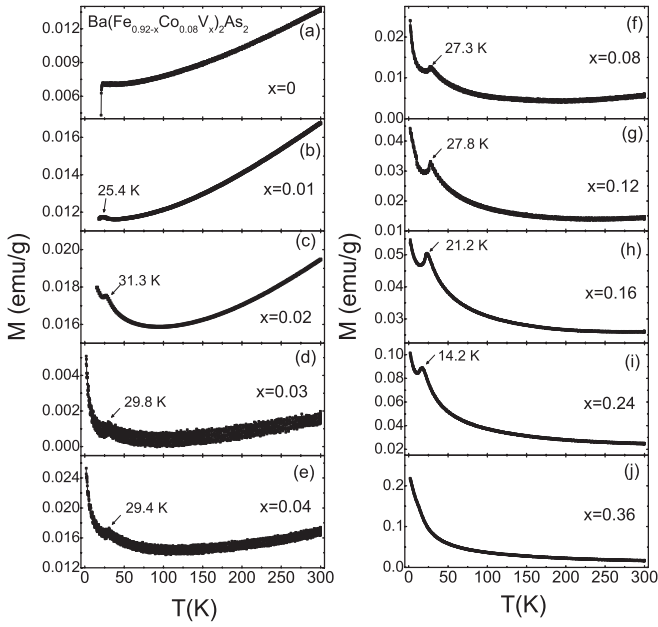


FIG. 2: (a)-(j) The temperature dependence of normal state DC susceptibilities for the $\text{Ba}(\text{Fe}_{0.92-x}\text{Co}_{0.08}\text{V}_x)_2\text{As}_2$ series under magnetic field of 1 T applied in the $\text{H}\parallel\text{ab}$ direction. The AFM transition temperatures T_N are determined from the dM/dT curves.

Fig. 2 is defined by the local extremum of the dM/dT curves, the resistivity anomaly temperatures could also be determined using the same method and have roughly the same values as T_N (see the final phase diagram in Fig. 5). It first increases slightly then decreases monotonously with doping until could not to be identified at $x=0.36$.

In order to further clarify the evolution of AFM order in $\text{Ba}(\text{Fe}_{0.92-x}\text{Co}_{0.08}\text{V}_x)_2\text{As}_2$, we performed elastic neutron scattering experiments on our samples using ‘Xingzhi’ and ‘Kunpeng’ cold neutron triple-axis spectrometers. Fig. 3(a) presents the \mathbf{Q} scans for AFM peak $\mathbf{Q}=(1\ 0\ 3)$ at $T=5\ \text{K}$ for $x=0.02, x=0.04, x=0.08, x=0.12, x=0.16, x=0.24$ and $x=0.32$ along \mathbf{H} direction. All the raw data of \mathbf{Q} -scans are subtracted by the background above T_N , the existence of magnetic peaks at $\mathbf{Q}_{AFM}=(1\ 0\ 3)$ is evident. The $(1\ 0\ 1)$ magnetic peaks were also collected for all the samples and their integrated intensities are approximately 45% of that for $(1\ 0\ 3)$ magnetic peaks. This intensity ratio is consistent with the calculations from a C -type AFM order in BaFe_2As_2 . For some samples, we also measured at least four nuclear peaks, combined with the two magnetic peaks, the magnetic ordered moment can be determined through the refinements using Fullprof software. As shown in Fig. 3(c), the ordered magnetic moments of $\text{Ba}(\text{Fe}_{0.92-x}\text{Co}_{0.08}\text{V}_x)_2\text{As}_2$ exhibit a strong dome-like doping dependent behavior with maximum value of $0.29\ \mu_B$, similar evolution of moments was also reported recently in Cr-doped $\text{BaFe}_{1.9-x}\text{Ni}_{0.1}\text{Cr}_x\text{As}_2$ [18].

To determine the spin-spin correlation length ξ , we fit all the $(1\ 0\ 3)$ magnetic peaks by Gaussian function as shown by the solid lines in Fig. 3(a). The values of ξ_{ab} for V-doped sam-

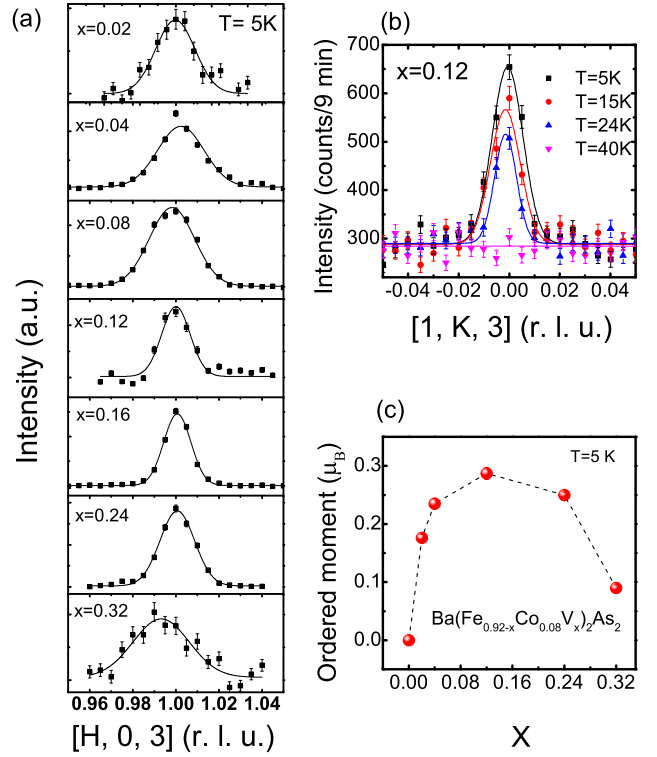


FIG. 3: (a) Longitudinal ($H\ 0\ 3$) scans at $\mathbf{Q}_{AFM}=(1\ 0\ 3)$ and $T=5\ \text{K}$. (b) Transverse ($1\ K\ 3$) scans at $\mathbf{Q}_{AFM}=(1\ 0\ 3)$ at different temperatures for $x=0.12$. (c) The ordered magnetic moments at $T=5\ \text{K}$ for $x=0, 0.02, 0.04, 0.12, 0.24$ and 0.32 .

ples from $x=0.02$ to $x=0.24$ are larger than $300\ \text{\AA}$. For some samples, such as $x=0.04$ and $x=0.16$, the L -scans for $(1\ 0\ 3)$ magnetic peak were also performed and fitted by Gaussian function (data not shown here), which give a similar result of $\xi_c > 300\ \text{\AA}$. The large values of ξ provide evidence for a long-range magnetic order has been restored for the V-doped samples. In addition, the temperature dependence of transverse \mathbf{K} -scan of $(1\ 0\ 3)$ magnetic peak for $x=0.12$ sample were also measured (shown in Fig. 3(b)). Through the Gaussian fit of these peaks, the magnetic peak is confirmed to be commensurate for all measured temperatures.

In order to further investigate the AFM and structural transitions, the temperature dependence of the intensities of nuclear Bragg peak $(2\ 0\ 2)$ and magnetic Bragg peak $(1\ 0\ 3)$ are studied for $\text{Ba}(\text{Fe}_{0.92-x}\text{Co}_{0.08}\text{V}_x)_2\text{As}_2$, respectively (shown in Fig. 4). For the tetragonal to orthorhombic structural transition, the neutron extinction effect from the peak splitting results in a significant change for the peak intensity of $(2\ 0\ 2)$ around the transition temperature. However, for $x \geq 0.24$, the huge structural factor and strong intensity of the Bragg peaks make it difficult to figure out the structural transition via extinction effect[18]. The structural transition temperatures T_S are roughly determined from the maximum slope of the change of $(2\ 0\ 2)$ intensity as shown in Fig. 4(a). The tem-

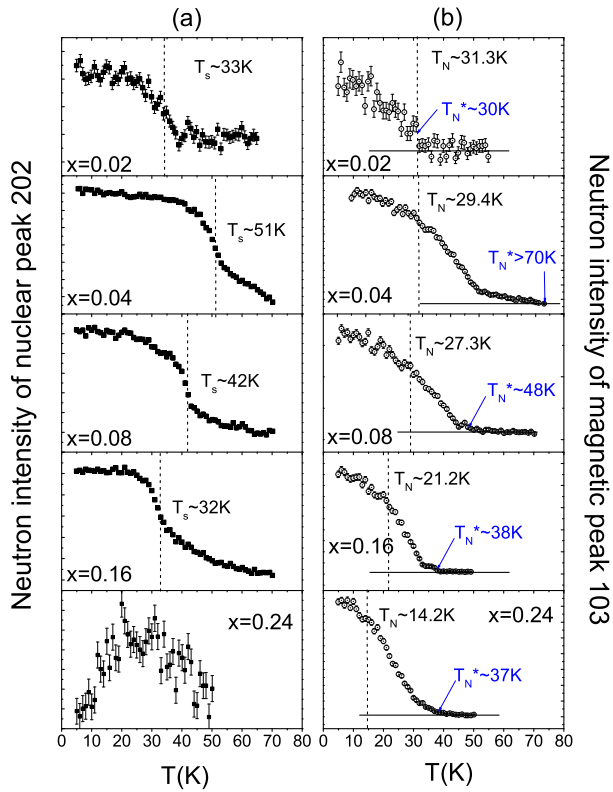


FIG. 4: Order parameters of structural and magnetic transitions in $\text{Ba}(\text{Fe}_{0.92-x}\text{Co}_{0.08}\text{V}_x)_2\text{As}_2$: (a) The temperature dependence of the neutron intensity at $Q=(2\ 0\ 2)$. (b) The temperature dependence of the neutron intensity at $Q_{AFM}=(1\ 0\ 3)$. T_N^* is defined as the onset temperature of $(1\ 0\ 3)$ peaks and the dotted lines represent the T_N determined from the susceptibility data.

perature evolutions of the magnetic order parameters are illustrated in Fig. 4(b). We notice that the magnetic order for most components can survive at much higher temperatures comparing with the T_N determined from susceptibility and resistivity measurement, especially for $x=0.04$, which exhibits a long magnetic intensity tail extending to $T=73\text{ K}$. In Fig.4(b), we define T_N^* as the onset temperature of the magnetic order from our neutron diffraction results and the dashed lines mark the T_N which is determined from the susceptibility data in Fig.2. Although for $x=0.02$ there is almost no difference between T_N^* and T_N , the deviations of T_N^* and T_N are quite obvious for $x \geq 0.04$. Finally in Fig. 5, the $x - T$ phase diagram of $\text{Ba}(\text{Fe}_{0.92-x}\text{Co}_{0.08}\text{V}_x)_2\text{As}_2$ is plot based on the experimental results above. We will discuss the features and underlying physics concerning to this phase diagram in the next section.

DISCUSSIONS AND CONCLUSIONS

The above experimental results confirm that the long-range commensurate magnetic order could be recovered through doping V into $\text{Ba}(\text{Fe}_{0.92-x}\text{Co}_{0.08}\text{V}_x)_2\text{As}_2$. The ordered mo-

ments of recovered AFM phases display a dome-like evolution versus x with maximum at $x=0.12$ (Fig. 3(c)). The similar recoveries of magnetic phase have been observed in Cr-doped $\text{BaFe}_{1.9-x}\text{Ni}_{0.1}\text{As}_2$ [18] and K-doped $\text{BaFe}_{2-x}\text{Co}_x\text{As}_2$ [19], which seems to be a universal phenomenon in FeAs-122 system but has never been realized in other unconventional magnetic superconducting system as far as we know. In our previous work[11], V is shown to act as an effective hole dopant similar as the cases of Cr and K. So a straightforward explanation about the recovery of magnetic order could be based on the Fermi surface nesting picture. Namely the introduction of holes into the electron doped FeAs-122 system compensates the charges by lowering the chemical potential and reshapes the Fermi surface. The better condition of Fermi surface nesting stabilizes the magnetic ordering, and further hole doping breaks the charge balance and finally diminishes the magnetic order. Although the Fermi surface nesting picture of the magnetism and superconductivity in many iron pnictides and iron chalcogenides materials has been challenged, it provides a good explanation for our experimental observations. The nature of magnetism in Fe-based superconductors remains elusive, the above observations of the charge tunable magnetic orders in FeAs-122 system should provide insights on the final physical picture.

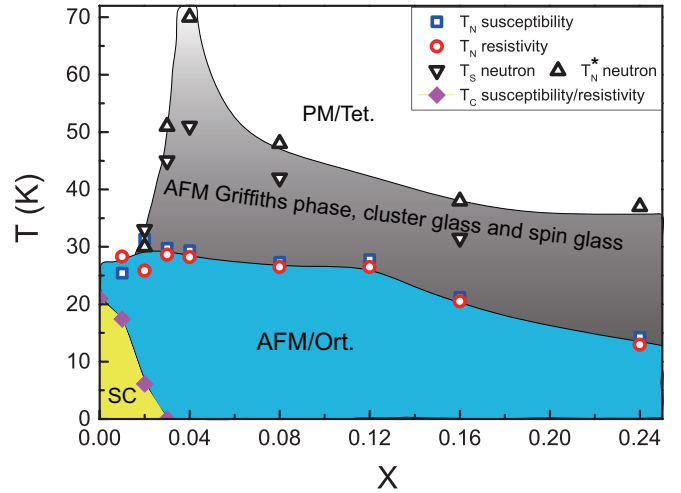


FIG. 5: $T-x$ phase diagram of $\text{Ba}(\text{Fe}_{0.92-x}\text{Co}_{0.08}\text{V}_x)_2\text{As}_2$ single crystals.

As shown in Fig.5, the AFM ordering temperatures T_N determined from susceptibility and resistivity data are consistent. They are around 14 K-30 K for all samples and exhibit a weak doping dependent behavior. However, neutron scattering experiments reveal that the magnetic peak $(1\ 0\ 3)$ has notable intensities at temperatures much higher than T_N for most samples. Especially for $x=0.04$, the intensity of magnetic peak exists even above 70 K, which is significantly larger than 29.4 K determined from the susceptibility data. The similar phenomenon has been previously reported by D. S. Inosov *et al.* in $\text{Ba}(\text{Fe}_{0.88}\text{Mn}_{0.12})_2\text{As}_2$ which is considered as an coexistence of AFM Griffiths phase[20], AFM clus-

ter glass and spin glass states in the region between T_N and T_N^* [21]. Normally these states would not generate sharp transition features in susceptibility and resistivity curves. But they can make notable slow dynamic contributions to the magnetic peak intensities which could be detected by neutron scattering measurements. Later, M. N. Gastiasoro *et al.* used a realistic five-band model with standard on-site Coulomb repulsion to study the magnetic order nucleated by magnetic impurities in iron pnictides[22]. They found that the magnetic tails of C -type AFM modulations close to the cores of magnetic impurities, may overlap with neighboring impurities and induce C -type AFM order even above T_N in a clear iron-pnictides system. This provides a microscopic explanation about the enhancement of C -type AFM ordering temperature in magnetic impurity doped iron pnictides. Similarly, impurity induced glassy clusters have been observed in the Fe(Te,Se) systems[23–25]. So based on the analysis above, our data strongly suggest the existence of the AFM Griffiths regime of multiple coexisting phases between T_N and T_N^* in the phase diagram of $\text{Ba}(\text{Fe}_{0.92-x}\text{Co}_{0.08}\text{V}_x)_2\text{As}_2$ as shown in Fig.5. Besides the similar T_N deviation between susceptibility and neutron data as reported in $\text{Ba}(\text{Fe}_{0.88}\text{Mn}_{0.12})_2\text{As}_2$ [21], another evidence is stated below. M. N. Gastiasoro *et al.*'s calculations[22] predict that the enhancement of C -type AFM order is strongly doping dependent, namely it occurs and reaches maximum above a certain doping concentration then gets weakened but always exists at higher doping (as shown in the Fig.1(e) of reference[22]). According to the phase diagram in Fig.5, the doping evolution of enhanced C -type AFM ordering temperature T_N^* agrees very well with the above theoretical prediction. Namely for $\text{Ba}(\text{Fe}_{0.92-x}\text{Co}_{0.08}\text{V}_x)_2\text{As}_2$, the enhancement of T_N^* starts at $x=0.03$ and suddenly reaches maximum at $x=0.04$, then gets weakened but always exists from $x=0.08$ to $x=0.24$. This consistency validates the physical picture provided by M. N. Gastiasoro *et al.* in explaining the phase diagram of $\text{Ba}(\text{Fe}_{0.92-x}\text{Co}_{0.08}\text{V}_x)_2\text{As}_2$, which reflects a cooperative behavior of the magnetic impurities and the conduction electrons mediating the Ruderman-Kittel-Kasuya-Yosida(RKKY) interactions between them. So far as we know, our observations seem to be the first experimental evidence for the theoretical predictions made by M. N. Gastiasoro *et al.* about the doping dependent behavior of magnetic impurities-enhanced AFM order. Most of the experimental reports about Griffiths-like phases are concerned with ferromagnetic materials[20], while the observations of such phases in antiferromagnets are very rare. So $\text{Ba}(\text{Fe}_{0.92-x}\text{Co}_{0.08}\text{V}_x)_2\text{As}_2$ could serve as a new system for further researches on exotic magnetic interactions.

In summary, the phase diagram of $\text{Ba}(\text{Fe}_{0.92-x}\text{Co}_{0.08}\text{V}_x)_2\text{As}_2$ has been investigated using x-ray, transport, magnetic susceptibility and neutron scattering measurements. The vanadium magnetic impurity could quickly suppress the superconductivity of $\text{Ba}(\text{Fe}_{0.92}\text{Co}_{0.08})_2\text{As}_2$ and restore a long-range commensurate C -type AFM order. The evolution of AFM ordered moments exhibits a dome-like behavior with V doping,

indicating a Fermi-surface nesting picture of magnetism in FeAs-122 system. On the other hand the evolution of doping dependent AFM ordering temperatures reveals the possible existence of AFM Griffiths phases, AFM cluster glass and spin glass in $\text{Ba}(\text{Fe}_{0.92-x}\text{Co}_{0.08}\text{V}_x)_2\text{As}_2$, which also provides as an experimental evidence for the previous theoretical prediction based on the RKKY interactions. The above results demonstrate the rich physics when vanadium magnetic impurities are introduced into iron pnictides superconductor, which may shed new light on understanding the Fe-based superconducting mechanism.

ACKNOWLEDGMENTS

This work is supported by the National Natural Science Foundation of China (No. 11227906 and No. 11204373). This work is also supported by the National Nature Science Foundation of China (No. 11875265), the Scientific Instrument Developing Project of the Chinese Academy of Sciences (3He based neutron polarization devices)the Institute of High Energy Physics, and the Chinese Academy of Science.

-
- [1] P. Dai, Rev. Mod. Phys. **87**, 855 (2015), URL <https://dx.doi.org/10.1103/RevModPhys.87.855>.
 - [2] W. Bao, Chin. Phys. B **22**, 087405 (2013), URL <https://dx.doi.org/10.1088/1674-1056/22/8/087405>.
 - [3] M. Rotter, M. Tegel, and D. Johrendt, Phys. Rev. Lett. **101**, 107006 (2008), URL <https://link.aps.org/doi/10.1103/PhysRevLett.101.107006>.
 - [4] Q. Huang, Y. Qiu, W. Bao, M. A. Green, J. W. Lynn, Y. C. Gasparovic, T. Wu, G. Wu, and X. H. Chen, Phys. Rev. Lett. **101**, 257003 (2008), URL <https://link.aps.org/doi/10.1103/PhysRevLett.101.257003>.
 - [5] D. K. Pratt, M. G. Kim, A. Kreyssig, Y. B. Lee, G. S. Tucker, A. Thaler, W. Tian, J. L. Zarestky, S. L. Bud'ko, P. C. Canfield, et al., Phys. Rev. Lett. **106**, 257001 (2011), URL <https://link.aps.org/doi/10.1103/PhysRevLett.106.257001>.
 - [6] X. Lu, H. Gretarsson, R. Zhang, X. Liu, H. Luo, W. Tian, M. Laver, Z. Yamani, Y.-J. Kim, A. H. Nevidomskyy, et al., Phys. Rev. Lett. **110**, 257001 (2013), URL <https://link.aps.org/doi/10.1103/PhysRevLett.110.257001>.
 - [7] F. Waßer, A. Schneidewind, Y. Sidis, S. Wurmehl, S. Aswartham, B. Büchner, and M. Braden, Phys. Rev. B **91**, 060505 (2015), URL <https://link.aps.org/doi/10.1103/PhysRevB.91.060505>.
 - [8] J. M. Allred, K. M. Taddei, D. E. Bugaris, M. J. Krogstad, S. H. Lapidus, D. Y. Chung, H. Claus, M. G. Kanatzidis, D. E. Brown, J. Kang, et al., Nat. Phys. **12**, 493 (2016), URL <https://dx.doi.org/10.1038/NPHYS3629>.
 - [9] K. Marty, A. D. Christianson, C. H. Wang, M. Matsuda, H. Cao, L. H. VanBebber, J. L. Zarestky, D. J. Singh, A. S. Sefat, and M. D. Lumsden, Phys. Rev. B **83**, 060509 (2011), URL <https://link.aps.org/doi/10.1103/PhysRevB.83.060509>.
 - [10] G. S. Tucker, D. K. Pratt, M. G. Kim, S. Ran, A. Thaler, G. E. Granroth, K. Marty, W. Tian, J. L. Zarestky, M. D.

- Lumsden, et al., Phys. Rev. B **86**, 020503 (2012), URL <https://link.aps.org/doi/10.1103/PhysRevB.86.020503>
- [11] X.-G. Li, J.-M. Sheng, C.-K. Tian, Y.-Y. Wang, T.-L. Xia, L. Wang, F. Ye, W. Tian, J.-C. Wang, J.-J. Liu, et al., Euro. Phys. Lett. **122**, 67006 (2018), URL <https://dx.doi.org/10.1209/0295-5075/122/67006>.
- [12] A. S. Sefat, G. D. Nguyen, D. S. Parker, M. M. Fu, Q. Zou, A.-P. Li, H. B. Cao, L. D. Sanjeewa, L. Li, and Z. Gai, Phys. Rev. B **100**, 104525 (2019), URL <https://link.aps.org/doi/10.1103/PhysRevB.100.104525>
- [13] P. Cheng, H. Zhang, W. Bao, A. Schneidewind, P. Link, A. Grnwald, R. Georgii, L. J. Hao, and Y. T. Liu, Nucl. Instrum. Methods A **821**, 17 (2016), URL <https://dx.doi.org/10.1016/j.nima.2016.03.045>
- [14] L. Y. Xing, X. Shi, P. Richard, X. C. Wang, Q. Q. Liu, B. Q. Lv, J.-Z. Ma, B. B. Fu, L.-Y. Kong, H. Miao, et al., Phys. Rev. B **94**, 094524 (2016), URL <https://link.aps.org/doi/10.1103/PhysRevB.94.094524>
- [15] R. Zhang, D. Gong, X. Lu, S. Li, P. Dai, and H. Luo, Supercond. Sci. Technol. **27**, 115003 (2014), URL <https://doi.org/10.1088%2F0953-2048%2F27%2F11%2F115003>
- [16] P. Cheng, B. Shen, J. Hu, and H.-H. Wen, Phys. Rev. B **81**, 174529 (2010), URL <https://link.aps.org/doi/10.1103/PhysRevB.81.174529>
- [17] N. Ni, M. E. Tillman, J.-Q. Yan, A. Kracher, S. T. Hannahs, S. L. Bud'ko, and P. C. Canfield, Phys. Rev. B **78**, 214515 (2008), URL <https://link.aps.org/doi/10.1103/PhysRevB.78.214515>.
- [18] D. Gong, T. Xie, R. Zhang, J. Birk, C. Niedermaier, F. Han, S. H. Lapidus, P. Dai, S. Li, and H. Luo, Phys. Rev. B **98**, 014512 (2018), URL <https://link.aps.org/doi/10.1103/PhysRevB.98.014512>
- [19] K. H. Zinth, V. Dellmann, T. and J. D., Angew. Chem. Int. Ed. **50**, 7919 (2011), URL <https://dx.doi.org/10.1002/anie.201102866>.
- [20] R. B. Griffiths, Phys. Rev. Lett. **23**, 17 (1969), URL <https://link.aps.org/doi/10.1103/PhysRevLett.23.17>
- [21] S. Inosov, G. Friemel, J. T. Park, A. C. Walters, Y. Texier, Y. Laplace, J. Bobroff, V. Hinkov, D. L. Sun, Y. Liu, et al., Phys. Rev. B **87**, 224425 (2013), URL <https://link.aps.org/doi/10.1103/PhysRevB.87.224425>
- [22] M. N. Gastiasoro and B. M. Andersen, Phys. Rev. Lett. **113**, 067002 (2014), URL <https://link.aps.org/doi/10.1103/PhysRevLett.113.067002>
- [23] W. Bao, Y. Qiu, Q. Huang, M. A. Green, P. Zajdel, M. R. Fitzsimmons, M. Zhernenkov, S. Chang, M. Fang, B. Qian, et al., Phys. Rev. Lett. **102**, 247001 (2009), URL <https://link.aps.org/doi/10.1103/PhysRevLett.102.247001>
- [24] L. D. Liu, J. Hu, B. Qian, D. Fobes, Z. Q. Mao, W. Bao, M. Reehuis, S. A. J. Kimber, K. Prokes, S. Matas, et al., Nature Materials **9**, 718 (2010).
- [25] V. Thampy, J. Kang, J. A. Rodriguez-Rivera, W. Bao, A. T. Savici, J. Hu, T. J. Liu, B. Qian, D. Fobes, Z. Q. Mao, et al., Phys. Rev. Lett. **108**, 107002 (2012), URL <https://link.aps.org/doi/10.1103/PhysRevLett.108.107002>